Relationship Between Mass Transfer Coefficient and Liquid Flow Velocity in Heterogenous Biofilms Using Microelectrodes and Confocal Microscopy

Paul Stoodley,[1] Shunong Yang,[2] Hilary Lappin-Scott,[1] Zbigniew Lewandowski[3].

[1]University of Exeter, Department of Biological Sciences, Hatherly Laboratories, Exeter, Devon EX4 4PS, United Kingdom; telephone: (44) 1392 264348; fax: (44) 1392 263700, e-mail: P.Stoodley@exeter.ac.uk
[2]NALCO Chemical Co., Napierville, Illinois
[3]Center for Biofilm Engineering, Montana State University, Bozeman, Montana 59717-3980

Received 20 November 1996; accepted 10 May 1997

Abstract: The relationship between local mass transfer coefficient and fluid velocity in heterogenous biofilms was investigated by combining microelectrodes and confocal scanning laser microscopy (CSLM). The biofilms were grown for up to 7 days and consisted of cell clusters separated by interstitial channels. Mass transfer coefficient depth profiles were measured at specific locations in the cell clusters and channels at average flow velocities of 2.3 and 4.0 cm/s. Liquid flow velocity profiles were measured in the same locations using a particle tracking technique. The velocity profiles showed that flow in the open channel was laminar. There was no flow at the top surface of the biofilm cell clusters but the mass transfer coefficient was 0.01 cm/s. At the same depth in a biofilm channel, the flow velocity was 0.3 cm/s and the mass transfer coefficient was 0.017 cm/s. The mass transfer coefficient profiles in the channels were not influenced by the surrounding cell clusters. Local flow velocities were correlated with local mass transfer coefficients using a semi-theoretical mass transfer equation. The relationship between the Sherwood number (*Sh*,) the Reynolds number (*Re*,) and the Schmidt number (*Sc*) was found using the experimental data to find the dimensionless empirical constants (*n*1, *n*2, and *m*) in the equation $Sh = n_1 + n_2 Re^m Sc^{1/3}$. The values of the constants ranged from 1.45 to 2.0 for n_1, 0.22 to 0.28 for n_2, and 0.21 to 0.60 for *m.* These values were similar to literature values for mass transfer in porous media. The Sherwood number for the entire flow cell was 10 when the bulk flow velocity was 2.3 cm/s and 11 when the bulk flow velocity was 4.0 cm/s. *Biotechnol Bioeng* **56:** 681–688, 1997.

Keywords: biofilm; confocal scanning laser microscopy; laminar flow; liquid flow velocity; mass transfer coefficient; microelectrodes; Reynolds number; Sherwood number

Correspondence to: Paul Stoodley
Contract grant sponsor: National Science Foundation
Contract grant number: EEC-8907039
Contract grant sponsor: Montana State University

INTRODUCTION

Although it has long been noted that biofilms may be heterogenous and have considerable surface roughness, they were generally conceptually thought of, and mathematically modeled, as planar structures (Picaloglou, et al. 1980; Siegrist and Gujer, 1985). These models assumed that diffusion was the main mass transfer mechanism inside the biofilm, convection was dominant in the bulk liquid outside the biofilm, and that mass fluxes were one dimensional, i.e., perpendicular to the substratum (Rittman and Manem, 1992; Siegrist and Gujer, 1985).

The recent application of confocal microscopy to biofilm research has led to a rethinking of the impact of structural heterogeneity on mass transfer and hydrodynamics (deBeer et al., 1994a,b; Gjaltema et al., 1994; Lawrence et al., 1991; Massol-Deya et al., 1994; Stoodley et al., 1994). It has been demonstrated, using Nuclear Magnetic Resonance Imaging, that water moves through channels in the biofilm (Lewandowski et al., 1994). This phenomena was quantified and the profiles of flow velocity measured using particle tracking in conjunction with confocal laser microscopy (deBeer et al., 1994b; Stoodley et al., 1994). Water movement inside the biofilm implies that the local mass transfer coefficient (*k*) may vary spatially. This was demonstrated by Yang and Lewandowski (1995) using a mass transfer coefficient microelectrode. They measured vertical and horizontal *k* profiles at specific locations in a biofilm by guiding the electrode microscopically. They found that the *k* varied from place to place in the biofilm, and concluded that this was caused by the structural heterogeneity of the biofilm. They also found a first-order relationship between local *k* in a biofilm void and the average velocity (*u*), but the coefficient of proportionality varied with depth.

Quantifying the relationship between *k* and *u* is an important step towards prediction of the macro-scale *k* based

 CCC 0006-3592/97/060681-08

on microscale measurements. Attempts to describe the relationship between k and u are not new in biofilm research but are normally measured over whole systems without regard for biofilm structure. Gantzer et al. (1988) found a logarithmic relationship between k and Reynolds number for chemical oxygen demand (COD) to an artificial streambed biofilm using a modification of a mass transfer equation for forced convection around a single sphere (Bird et al., 1960; Welty et al., 1969):

$$Sh = n_1 + n_2 Re^m Sc^{1/3} \quad (1)$$

where Sh is the Sherwood number, Re is the Reynolds number, Sc is the Schmidt number, and n_1, n_2, and m are constants. Similar forms of Equation (1) have been applied to flow through packed beds (Kennedy and Lennox, 1997). This mass transfer equation is particularly useful at low Re, when the n_1 term becomes significant and accounts for the limiting Sh that occurs when there is no flow. A more detailed review of mass transfer coefficient relationships can be found in a publication by Kennedy and Lennox (1997).

The goal of this work was to relate the local mass transfer coefficient to local liquid velocity in a heterogenous biofilm under laminar flow conditions. To do this, we combined the k microelectrode developed by Yang and Lewandowski (1995) with the particle tracking technique developed by Stoodley et al. (1994). This allowed us to compare the relationship between the mass transfer coefficient with liquid velocity on a scale relevant to the biofilm heterogeneity with literature values determined over entire reactor systems.

MATERIALS AND METHODS

Biofilm Reactor System

The flow cell was a closed channel (1 cm wide, 1 cm deep, and 45 cm long) with observation windows, 31 cm from the entrance, on the top and bottom surfaces (Stoodley et al., 1994). The windows were coverslips (60 × 24 mm), which were sealed in place by a rubber gasket and aluminum flange. The flow cell was placed in a recycle loop with a mixing chamber which had nutrient and dilution water influent streams delivered by peristaltic pumps (Masterflex, Cole-Parmer, Niles, IL). The mixing chamber was also aerated and had an overflow effluent line. The volume (V) of the mixing chamber and the recycle loop, including the flow cell, was approximately 140 mL. The flow cell could be placed on the stage of an inverted microscope (Olympus IMT-2) attached to a Bio-Rad MRC600 confocal scanning laser microscope (CSLM) without interrupting the flow conditions. This arrangement allowed the biofilm to be observed through the bottom window while at the same time, the top coverslip could be removed for microelectrode insertion (Fig. 1). The recycle flow rate (Q_R) was controlled using two vane head pumps (Masterflex, Cole-Parmer, Niles, IL), one at the inlet of the flow cell and the other at the outlet. The flow rate was monitored with an in-line flow meter (McMillan Flo-sensor model 101T supplied by Cole-Parmer, Niles, IL) or by volumetric displacement. During biofilm accumulation, the flow cell was operated as a closed channel with a flow rate of 3.5 cm^3/s (average flow velocity ($u_{(ave)}$) = Q_R/cross sectional area (CSA) = 3.5 cm/s). During the microelectrode and velocity measurements, the coverslip was removed and the flow cell became open channel. Measurements were taken at Q_R of 1.4 and 2.4 cm^3/s. At these flow rates, the water depth was 0.6 cm so that $u_{(ave)}$ were 2.3 and 4.0 cm/s, respectively.

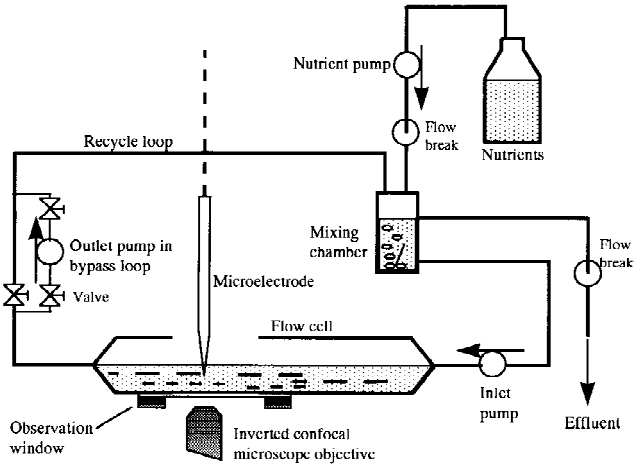

Figure 1. Reactor system showing the arrangement of the microelectrode, the inverted microscope, and the flow cell. During biofilm growth, the flow cell was operated as a closed channel and only the inlet pump used. When the microelectrode measurements were conducted, the top observation window of the flow cell was removed (as shown), and the outlet pump maintained at a slightly higher flow rate than the inlet pump to prevent overflowing. The dashed lines in the flow cell represent particle tracks used for the velocity measurement.

The Re based on the channel geometry were 258 and 448 calculated using:

$$Re = \frac{u_{(ave)} l}{\upsilon} \quad (2)$$

where υ was the measured kinematic viscosity of the electrolyte solution [0.972271 × 10^{-6} m^2/s at 20°C (Yang, 1995)] 1 was the characteristic length, which in this case, was the hydraulic diameter of the flow cell based on the wetted perimeter and cross-sectional area.

Nutrients were mixed with the dilution water in a ratio of 1:10 (0.7 mL/min:6.3 mL/min) for a final concentration of: glucose 40 ppm, potassium phosphate monobasic (KH_2PO_4) 70 ppm, potassium phosphate dibasic (K_2HPO_4) 30 ppm, ammonium sulfate [$(NH_4)_2SO_4$] 10 ppm, and magnesium sulfate ($MgSO_4 \cdot 7H_2O$) 1 ppm. The total nutrient influent flow rate (Q_N) was set at 7 mL/min to achieve a residence time ($\theta = V/Q_N$) of 20 min so that suspended cells would be washed out and biofilm growth favored.

The reactor and nutrient feed was sterilized by autoclaving at 121°C for 15 min. The dilution water was tap water

sterilized with in line capsule filters (1.0 μm prefilter and 0.1 μm filter), chlorine was removed by sparging with air. All experiments were performed at 20 ± 1°C.

Inoculum

Pseudomonas aeruginosa, Pseudomonas fluorescens, and *Klebsiella pneumoniae* were used to inoculate the reactor. The selection process for this consortium has been described earlier (Stoodley et al., 1994). Frozen stock cultures (1 mL) of each of the species were allowed to thaw, and then injected into the mixing chamber through a septum. The reactor was run as a batch culture for the first 24 h to allow the cells to attach before switching to continuous culture. Experiments were conducted on biofilms that were between 5 and 7 days old.

Biofilm Thickness Measurement and Depth Correction

The biofilm thickness (dimension in the plane perpendicular to the substratum) is defined in this study as the distance between the substratum and the peaks of the highest cell clusters. Using this definition, the channels (void fraction) that surround the cell clusters and streamers (biomass fraction) are considered integral components of the biofilm (Fig. 2). The height of the biofilm cell clusters were measured microscopically by focusing on the substratum (glass coverslip), and then moving the stage a known distance with a stepper motor until the surface of the cell cluster came into focus. Calibration of the stage stepper motor was required because the distance traveled by the stage was not the same as the distance between corresponding focal planes in the flow cell due to refraction effects of the air, glass, and water interfaces. Two methods were used to make the calibration: (1) the microscope was focused on the lower channel wall then refocused on the upper channel wall (an actual distance of 1 cm) using the stepper motor and the distance of travel was recorded—the ratio of the actual distance to the traveled distance was used to determine the correction factor; and (2) the microscope was focused on the microelectrode which was then moved up or down an assigned distance.

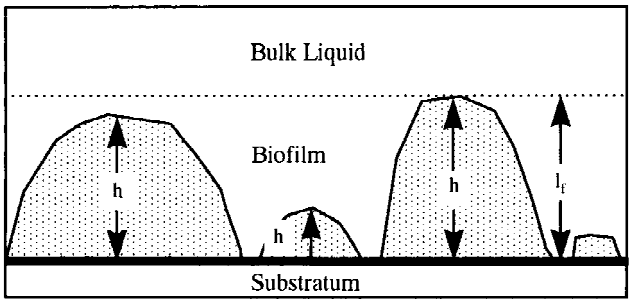

Figure 2. The biofilm thickness (l_f) is defined for this study as the distance between the substratum and the peaks of the highest cell clusters. The height (h) of the individual cell clusters is also indicated.

The microscope was next refocused on the microelectrode and the distance traveled by the stage was noted. The first method yielded a correction factor of 1.359, and the second 1.360. The distance traveled by the stage relative to the glass substratum was multiplied by 1.36 to find the depth of the focal plane in the flow cell. This was used to calculate the biofilm thickness and determine the depth position for the velocity profiles.

Measurement of Biofilm Surface Area Coverage and Length Dimensions

Image analysis was used to measure biofilm length dimensions (in the plane parallel to the substratum) and surface coverage. Processing was done on a Macintosh 7200/90 computer using the public domain NIH-Image 1.59 program (developed at the National Institutes of Health and available from the Internet by anonymous FTP from zippy.nimh.nih.gov or a floppy disk from the National Technical Information Service, Springfield, Virginia, part number PB95-500195GEI). A threshold was applied so that the biofilm cell clusters were black and the surrounding channels, white. The relative surface coverage of the biofilm was the proportion of black to total area. At the magnification used in this study, only the biofilm cell clusters, not the single cells on the glass surface, were included in the measurement. Length dimensions were measured using the ''line tool'' function. Length and area measurements were calibrated using a 1mm graticule with 10 μm divisions (Ref. # CS990, Graticules Ltd., Tonbridge, Kent, UK).

Mass Transfer Coefficient Measurements

The local k was measured in the flow cell with a microelectrode using the limiting current technique (LCT). The construction of the microelectrode, the LCT, and the experimental set-up as applied to biofilms has been described in detail by Yang and Lewandowski (1995). The tip diameter of each microelectrode was approximately 10 μm and was accurately measured microscopically. Because the microelectrode was mobile, k could be measured at specific locations in the biofilm under microscopic guidance by CSLM. Profiles of k in biofilm channels and clusters were made using a stepper motor. The method required that a redox couple was used in conjunction with the microelectrode. For these experiments, we used a reaction solution of potassium ferricyanide ($K_3Fe(CN)_6$, 25 m*M*) to provide the redox couple; $Fe(CN)_6^{+++}/Fe(CN)_6^{++}$, and potassium chloride (KCl, 0.5*M*) as a supporting electrolyte to suppress electromigration effects. Potassium ferricyanide was chosen because it is commonly used for electrochemical mass transfer measurements and does not react with the biofilm over the duration of the measurements (Selman and Tobias, 1978; Yang, 1995). Therefore, the ferricyanide concentration remains constant throughout the flow cell except at the tip of the electrode where it is consumed. Just before the k measurements were made, the nutrient solution was ex-

changed for the reaction solution which was added for 2 h (6 residence times) so that the reaction solution was essentially at 100% strength in the reactor. It has been shown that biofilm cells remain viable during exposure to the solution over the time taken to conduct the measurements (Yang and Lewandowski, 1995). The microelectrode was polarized cathodically with a counter calomel electrode (Model 13-620-51, Fisher Scientific, Pittsburgh, PA) to the limiting current value of −0.8 V. A Hewlett Packard 4140B multimeter was used as voltage source and picoammeter to measure the current (I) from the reduction of ferricyanide at the electrode surface. The mass transfer coefficient can be found from:

$$k = \frac{I}{nAFC_b} \tag{3}$$

in which n = the mole number of electrons transferred in the reaction (in this case 1), A is the electrode sensing area, F is Faraday's constant, and C_b is the bulk concentration of ferricyanide (Selman and Tobias, 1978).

The Sherwood number was calculated using:

$$Sh = \frac{kl}{D_c} \tag{4}$$

in which the characteristic length, l, was taken as the diameter of the microelectrode and D_c is the diffusion coefficient of ferricyanide in KCl solution. A D_c value of 7.3×10^{-10} m^2/s was reported by Konopka and McDuffie (1970) for ferricyanide (0.61 to 6.36 mM) in 1M KCl at 25°C and this value was used in this article, after correcting for the temperature difference using the Einstein Stokes equation. The Schmidt number was 1350.

Because of possible interference to the microelectrode from the wall of the flow cell, measurements were not made closer than one tip diameter from the wall.

Velocity Measurements

Liquid velocity measurements were made using a particle tracking technique described more fully elsewhere (Stoodley et al., 1994). Neutral density fluorescent latex spheres (Molecular Probes, Eugene, Oregon, density 20°C = 1055 kg/m^3, ex 580 nm/em 605 nm, diameter = 0.282 μm, 1.7×10^{12} spheres/mL) were added to the reactor to achieve a final concentration of about 1×10^7 particles/mL. When imaging with the CSLM, particles traveling across the field of view appeared as dashed lines on the screen. By measuring the length of these tracks (distance traveled) and the time taken to create the track, the velocity can be calculated. Velocity profiles in the flow cell were obtained by capturing images at various focal depths by raising or lowering the motorized stage. The actual depth was calculated from the apparent depth using the correction factor described in the preceding ''Biofilm Thickness Measurement'' section. The local Reynolds number was calculated using Equation (2) for correlation with local Sh. However, in this case the microelectrode diameter was used for the characteristic length so that the scaling factor would be the same for the two dimensionless groups.

Combined Mass Transfer Coefficient and Velocity Measurements

Because the particle tracking technique for measuring flow velocity (u) is non-intrusive and did not interfere with the k measurement, the two techniques were readily combined using CSLM. The electrode tip could be positioned at a specific point (in X,Y, and Z co-ordinates) in the biofilm and viewed with the CSLM. The particle tracking technique was then used to measure the liquid velocity at the same point. To avoid interference from the microelectrode on the liquid velocity, the k profile was measured before the u profile, although both were measured at the same X–Y location. It took between 2–5 min to measure a k profile and about 5 min to capture the sequence of images required to construct a u profile. Combined u and k profiles were measured in biofilm clusters and channels.

Although k and u profiles were measured at the same X–Y location, the depth (Z) positions did not always coincide, because they were determined by different methods, i.e., the stepper motor for the k and the focus motor for the u. To view the data graphically and correlate Sh with Re, a k value and corresponding u value was required at the same depth. To achieve this, the velocity profiles were fitted to a curve with TableCurve 2D for Windows (Jandel Scientific, San Rafael, CA), and the resulting polynomial equations used to find the corresponding u at the same depth as the measured k value.

Correlations and Statistics

The Sh was related to the Re according to Equation (1) using a linearization method described by Gantzer et al. (1988) to find the constants n_1, n_3, and m. The goodness of fit of the experimental data to the model data was estimated by linear regression. A sensitivity analysis of Equation (1) was performed using a representative set of constants at a Re of 0.1 to determine the relative contributions of each constant to the overall prediction value of the model. Each constant was individually varied, and the absolute percent change of the predicted value calculated.

RESULTS

Biofilm Accumulation

After 5 days, the biofilms consisted of cell clusters separated by surrounding water channels (Fig. 3). The structure was similar to that reported previously (deBeer et al. 1994a,b; Stoodley et al. 1994). The largest cell clusters were close to hemispherical in shape and ranged in height from 175–225 μm. The diameter of the cell clusters at the base of

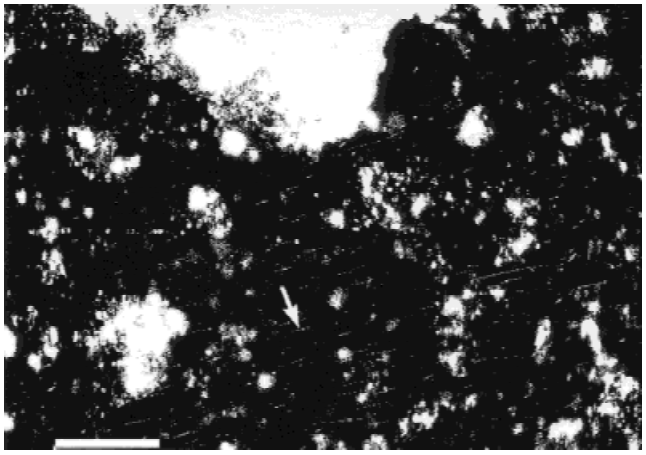

Figure 3. Plan view of the biofilm composed of cell clusters (white) and surrounding channels (black). The white dashes in the channels are tracks made by fluorescent particles used for the velocity measurements (a representative track is shown by the arrow). The bulk flow was from right to left. Mass transfer coefficient and velocity profiles were measured in the large void area in the center of the image. The scale bar is 100 μm (bottom left corner).

the biofilm ranged from 10 to 500 μm. The width of the water channels were of the same order. The surface coverage of the cell clusters was 41.7% (standard error = 5.6, n = 3). Some single cells were observed on the substratum in the biofilm void areas. There was no appreciable difference in the structure of the 7 day-old biofilms. Replacement of the nutrients with potassium ferricyanide and potassium chloride solution for the k measurement had no affect on the biofilm structure.

Mass Transfer Coefficient Profiles

$u_{(ave)}$ = 4.0 cm/s

Mass transfer coefficient profiles were measured in three biofilm channels at this velocity. The profiles were parabolic as k decreased from around 0.027 cm/s at a depth of 1.5 mm to 0.012 cm/s at a depth of 10 μm (Fig. 4). The rate of decrease of k became greater as the substratum was approached. The k at the top of the biofilm was approximately 0.020 cm/s. There was no perturbation to the profiles in the region of the surrounding cell clusters.

$u_{(ave)}$ = 2.3 cm/s

At this flow velocity, profiles were measured in both channels and cell clusters. In the void, the profile was similar to those measured at the higher flow rate, and went from approximately 0.021 cm/s at a depth of 2 mm to 0.014 cm/s at a depth of 10 μm (Fig. 5a) in a smooth parabola. However, in the cluster, the curve was perturbed near the surface of the cell cluster, at a depth of 170 μm (Fig. 5b). The k at the surface of the cluster was 0.01 cm/s, then just below the surface of the cluster there was a slight increase to 0.012

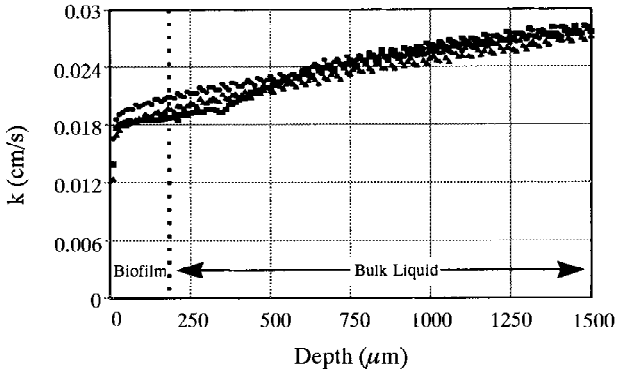

Figure 4. Mass transfer coefficient profiles in three different biofilm channels at a bulk liquid average flow velocity of 4.0 cm/s (flow cell Re = 448). Data points for each set are distinguished by symbol type. The position of the top of the surrounding biofilm cell clusters is indicated by the dashed line. The substratum is at depth = 0.

cm/s at 150 μm, before again rapidly decreasing at the substratum. The k at the same depth in the channel was 0.017 cm/s. The k decreased at a similar rate as the surface of the cell cluster was approached as that when approaching the substratum in a void.

Velocity Profiles

Velocity profiles were measured in cell clusters and void areas of the biofilm. Above the cell cluster, there was a

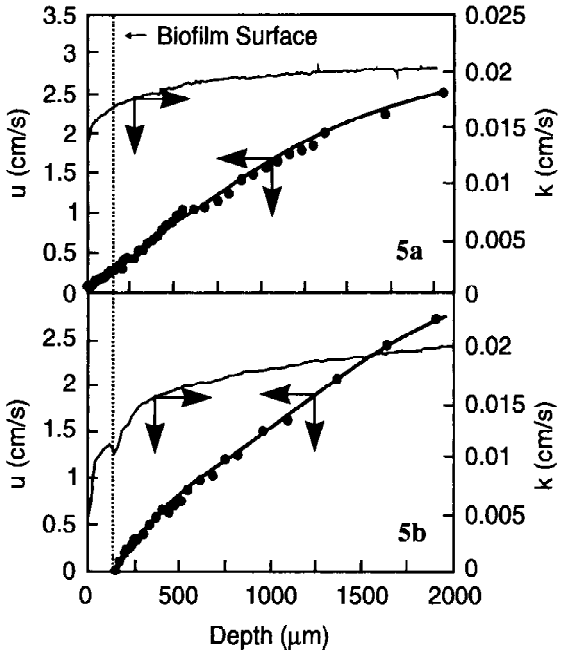

Figure 5. Velocity (u) and mass transfer coefficient (k) profiles measured in a biofilm void (a), and a biofilm cluster (b), at an average flow rate of 2.3 mL/s (flow cell Re = 250). In the void, both curves were parabolic but the velocity profile was much steeper (note the different scales). The surrounding biofilm clusters did not appear to effect the profile. In the cell cluster, the velocity went to zero at the top of the cluster, which was at depth of about 170 μm. The mass transfer coefficient increased slightly at the top of the cluster, indicating that there was a slight increase in mixing in this region.

shadow region extending for about 1 mm from the top of the cluster in which the particles could not be seen. It is not known why this occurred. However, we were able to construct a complete profile at the edge of one of the clusters, in addition, three profiles were constructed in void areas. The velocity profiles were parabolic indicating laminar flow, as expected from the *Re* based on the flow cell geometry (Figs. 5a,b). In the channels, there was liquid flow down to the glass substratum. At $u_{(ave)}$ of 2.3 cm/s, local flow in the void increased from 0 cm/s at the substratum to about 0.3 cm/s at the top of the biofilm. The velocity then continued to increase to about 3 cm/s at a depth of 3.5 mm. There was a slight break in the profile at the top of the biofilm, indicating a lower shear rate through the biofilm than immediately outside it. The liquid flow went to zero at the top surface of the cluster which was about 170 μm above the substratum.

The three velocity profiles measured at $u_{(ave)}$ of 4.0 cm/s (data not shown) used for correlation with the *k* profiles were also parabolic, and were all fitted with TableCurve to fifth-order polynomial equations with r^2 correlations greater than 0.998.

Relationship Between *u* and *k*

The curve fitting equations of the velocity profiles were used to pair *u* and *k* values at equal depths in the flow cell. For these correlations the dimensionless groups, the Reynolds number, and Sherwood number were used respectively. The curves were generally parabolic, and the rate of increase in *Sh* decreased as *Re* increased. A representative data set and the corresponding model curve are shown in Figure 6. The predicted values of *Sh* from the model were compared with the experimental data using linear regression. Table I shows the solution for the constants and the results from the regression analysis for the three data sets.

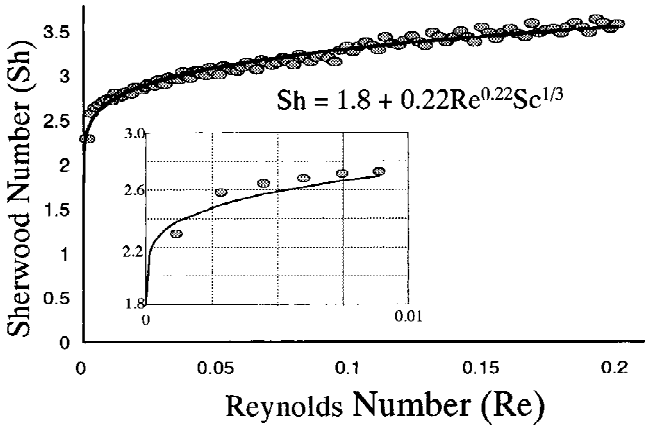

Figure 6. Variation of local Sherwood number with local Reynolds number measured in a biofilm void at an average flow velocity of 4.0 cm/s. The measured data (circles) were used to determine the constants in the model equation indicated on the graph. The curve generated by the model is shown by solid line. The inset shows greater detail of the intercept region.

Table I. Solutions for the constants n_1, n_2, and *m* in the mass transfer equation [Eq. (1)] for the three data sets shown in Figure 4. The regression correlation coefficient (r^2) is shown with the corresponding standard error (SE); there were 100 data points for each data set.

	n_1	n_2	*m*	r^2	SE
Data set 1	1.80	0.22	0.22	0.96	0.00159
Data set 2	1.45	0.27	0.21	0.96	0.00239
Data set 3	2.30	0.28	0.60	0.97	0.00153

A sensitivity analysis was performed on data set 1 to determine the effect of each of the constants on the predicted *Sh*. Only one constant was varied at a time while the other two constants were kept at their original values. The n_l constant had the largest influence on the resulting *Sh*, and on *m* the least influence, although all three were of the same order (Table II).

DISCUSSION

Mass Transfer Coefficient Depth Profiles Measured in Biofilm Channels

The profiles ran smoothly from the bulk liquid to the substratum in the void areas of a flow cell colonized with a 200 μm thick biofilm. Because the surrounding biofilm clusters did not have a significant influence on the profiles, it may be assumed that there was also little effect on mixing in the channels. In this case, one dimensional models may adequately describe the mechanism of mass transfer. This finding is consistent with earlier work by deBeer et al. (1996), which found that biofilm channels only facilitated the mass transfer of nutrients when the average velocity approached 11.5 cm/s (*Re* = 800).

Although we used a microelectrode to investigate the effect of local heterogeneity on mass transfer for practical purposes, it is more useful to determine an overall *k* to describe substrate removal. We used the *k* measured by the microelectrode near the surface of the cell clusters for comparison with other results. Although the microelectrode is measuring *k* from the bulk fluid to the tip of the electrode, it is reasonable to expect that the *k* measured near the surface of the biofilm would be similar to that for a substrate being consumed by a biofilm under transport limitation, because the transport conditions would also be similar. The *k* values that we measured at the top of the biofilm (1.0–2.0 × 10^{-2} cm/s at *Re* of 448) were about half an order of

Table II. Percent change on the predicted *Sh* when half (50%) and twice (200%) the original value of the empirical constants n_1, n_2, and *m* were varied in the mass transfer equation [Eq. (1)].

% of original constant value	n_1	n_2	*m*
50	27	23	13
200	55	45	18

magnitude greater than those measured by Siegrist and Gujer (1987) (2.3×10^{-3} cm/s for oxygen in a biofilm colonized trickling filter under laminar conditions) and Gantzer et al. (1988) (0.58×10^{-3} cm/s for COD removal by a gravel bed biofilm at a shear *Re* of 441). The reaction rate of bacterial cells in a biofilm may be nutrient limited as well as transport limited, whereas the reaction rate at the tip of the electrode is only transport limited. As such, it may be expected that the *k* value from the microelectrode is a maximum for a certain flow condition. An overall *Sh* of 11 was calculated using Equation (1) with the constants from data set 1 at a *Re* of 448 based on the flow cell geometry. When the *Re* was 258, the *Sh* was 10. From these *Sh,* an overall *k* can be calculated, but it is not clear what should be used as the characteristic length in this case. When the hydraulic diameter of the flow cell is used as the characteristic length, a *k* value of 7.3×10^{-5} cm/s is obtained. However, if the electrode diameter is used, then *k* becomes 8.0×10^{-2} cm/s. Clearly, care must be taken in the choice of the characteristic length, and further experiments are required to investigate relationships between measurements made at the micro scale and overall mass transfer coefficients. Possibly, a characteristic length based on channel width would be more appropriate because nutrients are transported to the surface of the cell clusters from the channels.

Combined Mass Transfer Coefficient and Velocity Depth Profiles

We were able to measure *k* and *u* profiles almost simultaneously by combining the electrode and particle tracking techniques. In addition, use of the confocal microscope allowed us to measure these profiles at specific locations in the biofilm. Although the velocity went to zero at the surface of the cell clusters, there was a slight increase in the local *k.* A similar increase at the cell cluster–bulk liquid interface has been previously reported (Yang, 1995). Although this small increase would probably not have any significant effect on the overall *k,* it may indicate mixing in this region, possibly from vibration of the biofilm. At higher flow rates, this effect may become more pronounced due to vortex shedding from the cell clusters with significant consequences for momentum, heat and mass transfer (Lewandowski and Stoodley, 1995). It is also possible that the increase was an artifact induced by the contact of the microelectrode with the surface of the cell cluster. Inside the cluster, the *k* continued to slowly decrease as the substratum was approached, indicating that mass transfer inside the cluster was similar to that in the surrounding channels. It is possible that this mixing in the clusters was caused by convection in microchannels, as suggested by Yang and Lewandowski (1995).

The curve fitting technique applied to the mass transfer equation [Eq. (1)] determined that *Sh* was proportional to *Re* raised to a power ranging from 0.21 to 0.60. Literature values show that this exponent ranges from 0.33 at $Re = 0$ to 0.66 as *Re* tends to infinity (Kennedy and Lennox, 1997). The constant n_2 ranged between 0.22 to 0.28. Literature values of between 0.552 and 1.1 are reported for this constant (Bird et al., 1960; Kennedy and Lennox, 1997). The dimensionless n_1 ranged from 1.45 to 2.30 with an average value of 1.85. When there is no convection, $Re = 0$ and $Sh = n_1$. Our value is close to literature values which show that when there is no flow, $Sh = 2$ (Bird et al., 1960; Kennedy and Lennox, 1997). The n_1 constant had the greatest influence on the predicted *Sh.*

Regression analysis showed that there was a good correlation between the mass transfer equation [Eq. (1)] using the solved constants and the experimental data. The r^2 values for the three data sets were all greater than 0.96. The mass transfer equation used in this study was initially formulated to describe heat transfer from the surface of a sphere in an infinite medium. However, it has since been adapted to mass transfer using the Chilton–Colburn analogy (Bird et al., 1960), and has been applied to low *Re* flow through packed beds (Kennedy and Lennox, 1997). Heterogenous biofilms have similarities to porous media (the channels may be considered the void fraction), and water flow through the biofilm will often be at very low Reynolds numbers (the characteristic length of the channels is small as is the liquid velocity because the biofilm is usually in the hydrodynamic boundary layer). Our data indicate that Equation (1) may also be successfully applied to describe mass transfer processes occurring in heterogenous biofilms.

CONCLUSIONS

1. Measurement of mass transfer coefficient by microelectrode can be combined with the particle tracking technique and CSLM to study the relationships between mass transfer, liquid convective flow, and biofilm structure on the microscale.
2. The velocity and mass transfer coefficient profiles were parabolic, approaching a plateau in the bulk flow and becoming asymptotic to zero at the wall.
3. At the applied flow velocities the heterogenous biofilm structure had no significant effect on the local mass transfer coefficient in the biofilm channels.
4. The local Sherwood number could be related to the local Reynolds number using the equation $Sh = n_1 + n_2\, Re^m\, Sc^{1/3}$ where n_1, n_2, and m are constants found from linearization curve fitting.

From Montana State University, we thank Fuhu Xia and Kjetil Rasmussen for their experimental help, and Peg Dirckx for editorial assistance. From Exeter University, we thank John Boyle and Mick Wheelan for their technical advice.

NOMENCLATURE

C_s	concentration of reacting electrolyte at the electrode surface (Mole/m^3)
d	depth (L)
D_C	diffusion coefficient of ferricyanide in KCl solution (L^2/T)
D_e	effective diffusion coefficient (L^2/T)

D_w	diffusion coefficient in water (L^2/T)
F	Faraday constant (9600 coulombs/mole)
h	height (L)
I	current (ampere or coulombs/second)
k	mass transfer coefficient (L/T)
l	characteristic length (L)
l_f	biofilm thickness
m	empirical constant (dimensionless)
n	number of moles of electrons transferred (dimensionless)
n_1,n_2	empirical constants (dimensionless)
Q_N	nutrient flow rate (L^3/T)
Q_R	recycle flow rate (L^3/T)
r^2	regression correlation coefficient (dimensionless)
Re	Reynolds number (dimensionless)
Sc	Schmidt number (dimensionless)
Sh	Sherwood number (dimensionless)
u	flow velocity (L/T)
$u_{(ave)}$	average flow velocity (L/T)
V	volume (L^3)
θ	hydraulic residence time (T)
υ	kinematic viscosity (L^2/T)

References

Bird, R. B., Stewart, W. E., Lightfoot, E. N. 1960. Transport phenomena, pp. 407–415, 642–648. Wiley, New York.

deBeer, D., Stoodley, P., Roe, F., Lewandowski, Z. 1994a. Effects of biofilm structures on oxygen distribution and mass transfer. Biotechnol. Bioeng. **43**: 1131–1138.

deBeer, D., Stoodley, P., Lewandowski, Z. 1994b. Liquid flow in heterogenous biofilms. Biotechnol. Bioeng. **44**: 636–641.

deBeer, D., Stoodley, P., Lewandowski, Z. 1996. Liquid flow and mass transfer in heterogeneous biofilms. Water Res. **30**: 2761–2765.

Gantzer, C. J., Rittman, B. E., Herricks, E. E. 1988. Mass transfer to streambed biofilms. Water Res. **22**: 709–722.

Gjaltema, A., Arts, P. A. M., van Loosdrecht, M. C. M., Kuenen, J. G., Heijnen, J. J. 1994. Heterogeneity of biofilms in rotating annular reactors: Occurrence, structure, and consequences. Biotechnol. Bioeng. **44**: 192–204.

Kennedy, C. A., Lennox, W. C. 1997. A pore-scale investigation of mass transport from dissolving DNAPL droplets. Journal of Contam. Hydrol. **24**: 221–246.

Konopka, S., McDuffie, B. 1970. Diffusion coefficients of ferri-and ferrocyanide ions in aqueous media, using twin-electrode thin-layer electrochemistry. Anal. Chem. **42**: 1741–1746.

Lawrence, J. R., Korber, D. R., Hoyle, B. D., Costerton, J. W., Caldwell, D. E. 1991. Optical sectioning of microbial biofilms. J. Bacteriol. **173**: 6558–6567.

Lewandowski, Z., Stoodley, P., Altobelli, S., Fukushima, E. 1994. Hydrodynamics and kinetics in biofilm systems—Recent advances and new problems. Water Sci. Technol. **29**: 223–229.

Lewandowski, Z., Stoodley, P. 1995. Flow induced vibrations, drag force, and pressure drop in conduits covered with biofilm. Water Sci. Technol. **32**: 19–26.

Massol-Deya, A. A., Whallon, J., Hickey, R. F., Tiedje, J. M. 1994. Channel structures in aerobic biofilms of fixed-film reactors treating contaminated groundwater. Appl. Environ. Microbiol. **61**: 769–777.

Picologlou, B. F., Zelver, N., Characklis, W. G. 1980. Biofilm growth and hydraulic performance. J. Hydraul. Div. Am. Soc. Civ. Eng. **106**: 733–746.

Rittman, B. E., Manem, J. A. 1992. Development and experimental evaluation of a steady state, multispecies biofilm model. Biotechnol. Bioeng. **38**: 914–922.

Selman, J. R., Tobias, C. W. 1978. Mass transfer measurements by the limiting-current technique. pp. 211–315. In: T. B. Drew, G. R. Cokelet, J. W. Hoopes, and T. Vermeulen (eds.). Advances in chemical engineering, vol 10. Academic Press, New York.

Siegrist, H., Gujer, W. 1985. Mass transfer mechanisms in a heterotrophic biofilm. Water Res. **19**: 1369–1378.

Siegrist, H., Gujer, W. 1987. Demonstration of mass transfer and pH effects in a nitrifying biofilm. Water Res. **21**: 1481–1487.

Stoodley, P., deBeer, D., Lewandowski, Z. 1994. Liquid flow in biofilm systems. App. Env. Micro. **60**: 2711–2716.

Welty, J. R., Wilson, R. E., Wicks, C. E. 1969. Fundamentals of momentum, heat and mass transfer, pp. 578–591. Wiley, New York.

Yang, S. 1995. Microelectrode measurement of local mass transfer coefficient in biofilms. M.S. thesis, Montana State University, Bozeman, MT.

Yang, S., Lewandowski, Z. 1995. Measurement of local mass transfer coefficient in biofilms. Biotech. Bioeng. **48**: 737–744.